Distribution of dust color temperature, dust mass and Planck's function around C-rich AGB star: IRAS 19558+3333 using IRIS, AKARI, and WISE surveys

R. Kandel*, A. Chaudhary, K. Chaudhary**, M. Jalan**, A. Subedi*, K. Khatiwada*, D. R. Upadhyay*,**and A. K. Jha****

*Department of Physics, Amrit Campus, Tribhuvan University, Kathmandu, Nepal.

**Central Department of Physics, Tribhuvan University, Kathmandu, Nepal.

Abstract: The dust properties of C-rich AGB (Asymptotic giant branch) star IRAS 19558+3333 located at right ascension (R.A.) (J2000) = $19^h\ 57^m\ 48.440^s$ and Declination (J2000) = $+33^0\ 41^m\ 21.250^s$ was studied. The FITS image of this AGB star was obtained by SkyView Virtual Observatory in IRIS, AKARI, and WISE surveys respectively. The flux of ambient medium in the wavelength range of IRIS 60 μm and 100 μm, AKARI 90 μm and 140 μm and WISE 12 μm and 22 μm was calculated along with the physical properties like dust color temperature, dust mass, Planck's function and visual extinction of the candidate at a distance of 3415.420 pc. The minimum and maximum dust mass is found to be 1.606× 10^{21} kg (8.030 × 10^{-10} M⊙), and 7.013 × 10^{20} kg (3.506× 10^{-10} M⊙) in IRIS, 2.739 × 10^{22} kg (1.369× 10^{-8} M⊙), and 1.292 × 10^{22} kg (6.460 × 10^{-9} M⊙) in AKARI and 2.297 × 10^{20} kg (1.148 × 10^{-10} M⊙) and 3.013 × 10^{19} kg (1.506 × 10^{-11} M⊙) in the WISE survey and the dust color temperature of the corresponding C-rich star average value was found to be 24.230 ± 0.229 K in IRIS, 16.780 ± 0.189 K in AKARI and 123.750 ± 0.430 K in WISE survey. The temperature in WISE was higher than that of the AKARI and WISE surveys.

Keywords: Dust color temperature; dust mass; interstellar medium; Planck's function.

Introduction

Interstellar matter accounts for nearly 15% of visible matter in our galaxy. ISM is composed of approximately 91% hydrogen, 8.9% helium, and 0.1% heavier elements other than hydrogen or helium. The ISM is divided into several phases that are distinguished by their densities, temperatures, and ionization fractions[1-3].

Asymptotic giant branch (AGB) stars are classified as either oxygen-rich or carbon-rich or silicon-rich based on the chemistry of their photosphere. In terms of properties, S stars are thought to be somewhere between O-rich and C-rich stars. The mass loss of AGB occurs at the end of its lifetime. Over the last decade, several exciting aspects of AGB evolution have been revealed. There are two types of AGB stars: those that have not yet begun the thermal pulsing phase, known as early-AGB stars, and those that have begun the thermal pulsing phase, known as TP-AGB stars. The AGB star's mass-losing stages were adjusted to account for the effect of dust. There are various (1168) objects of C-rich AGB stars discovered[4-6].

Jha and Aryal studied the properties of interstellar dust using the infrared survey in the region near the Pulsars[7], Jha & Upadhyay studied dusty environments nearby AGB Star[8] and calculated dust temperature. Dust color temperature, Planck's function have been determined by a few researchers nearby Far Infrared (FIR) loops[9], FIR Cavities[10]. Gautam and Aryal[11] reported a Study of a far

Author for correspondence: Ajay Kumar Jha, Central Department of Physics, Tribhuvan University, Kathmandu, Nepal.
Email: astroajay123@gmail.com

Received: 13 May 2023; Received in revised form: 16 June 2023; Accepted: 20 June 2023.
Doi: https://doi.org/10.3126/sw.v16i16.56833

infrared cavity surrounding a post-AGB star under IRAS survey at galactic latitude -3^0 in earlier pertinent study. By utilizing the IRAS survey, they have studied many physical characteristics such as dust temperature, mass, and inclination angle. The dust color temperature and visual extinction distribution of a far infrared cavity at 60 μm and 100 μm IRAS map around the AGB star at galactic latitude 8.6° were also studied by Gautam and Aryal[12]. Gautam and Aryal[13] also investigated the visual extinction near the AGB star at latitude 1.6° of the galaxy. Gautam and Chhatkuli[14] and Joshi et al.[15] have conducted related research at various galactic latitudes.

Because of the fascinating nature of the ISM and AGB stars, we will take a broad and extended approach to each of the related topics, excavating the physics behind each physical property. Our work includes estimating the dust color temperature, dust mass, spectral density, and radiation intensity of a C-rich AGB star, and determining the type of AGB star, providing a broad area for studying the interaction of AGB stars and ISM matter.

Materials and method

The source name, right ascension, declination, and other characteristics were obtained via the Gaia archive (https://gea.esac.esa.int/archive/). The source coordinates were found using SIMBAD (https://simbad.u-strasbg.fr/simbad/sim-fid) and Sky View Virtual Observatory (https://skyview.gsfc.nasa.gov/current/cgi/titlepage.pl) used those coordinates as input. We have downloaded our candidate's JPEG and FITS images at several wavelengths, such as 12 μm and 24 μm in WISE, 60 μm and 100 μm in IRIS, and 90 μm and 140 μm in AKARI. Aladin V2.5 and V11.5 were used to examine each pixel of the FITS images. After obtaining the flux value for each pixel in the FITS image, further calculations were done.

Dust Temperature

We have used the method of Dupac et al.[16] and Schnee et al.[17] to calculate the dust Color Temperature.

For IRIS:

The expression to calculate the dust color temperature for IRIS[18] survey is:

$$T_d = \frac{-96}{ln\left[R\times 0.64^{(3+\beta)}\right]} \quad \text{……..…..(1)}$$

Where, flux density ratio, R, is given by:

$$R = \frac{F(60\mu m)}{F(100\mu m)} \quad \text{…..... (2)}$$

The flux densities at 60 μm and 100 μm, respectively, are F(60 μm) and F(100 μm). The spectral emissivity index value, β, is determined by dust particle parameters such as composition, size, and compactness.

Here, $\beta = \frac{1}{(\delta+\omega T)}$

Where δ and ω are free parameters.

A pure black substance has a value of β =0, amorphous layer lattice matter has a value of β =1, and crystalline dielectric has a value of β =2[16,18]

For AKARI:

The expression for dust color temperature in the AKARI survey is:

$$T_d = \frac{-57}{ln\left[R\times 0.64^{(3+\beta)}\right]} \text{.....(3)}$$

Where, flux density ratio, R, is

$$R = \frac{F(90\mu m)}{F(140\mu m)} \quad \text{…..…..(4)}$$

Here, F(90μm) and F(140μm) are the flux densities at 90 μm and 140 μm respectively.

For WISE:

The expression for dust color temperature in the WISE survey is:

$$T_d = \frac{-546}{ln\left[R\times 0.64^{(3+\beta)}\right]} \text{.....(5)}$$

Where, flux density ratio, R, is

$$R = \frac{F(12\mu m)}{F(22\mu m)} \text{.....(6)}$$

Planck's Function

The Planck's function is a well-known function, given by this equation,

$$B(\upsilon, T_d) = \frac{2h\upsilon^3}{c^2}\left[\frac{1}{e^{\left(\frac{h\upsilon}{k_B T_d}\right)}-1}\right] \text{.....(7)}$$

where,

h = Planck's constant, c = velocity of light, ν = frequency at which the emission is observed, and T_d the average temperature of the region[15].

Dust mass

The dust mass is estimated from the IR flux densities. The resulting dust mass depends on the physical and chemical properties of the dust grains, the adopted dust color temperature (T_d) and the distance (D)[20-21]. For the calculation of dust mass, first we need the value of flux density F_v,

F_v=NB(υ , T_d)Q(ν) $\frac{\pi a^2}{D^2}$ .....(8)

Where Q(ν) is grain emissivity index. The dust mass can be calculated as,

M_d=$\frac{4\alpha\rho}{3Q(\nu)}\frac{F(\nu)D^2}{B(\nu,T_d)}$ .....(9)

Here, α = weighted grain size, ρ = grain density, Q (ν) = grain emissivity,

F(ν) = f ×MJy/sr ×5.288× 10^{-9}, where 1 MJy/sr =1× 10^{-2} kg s^{-2} and f = relative flux density measured from the image[20] .

Results and Discussion

Map Projection

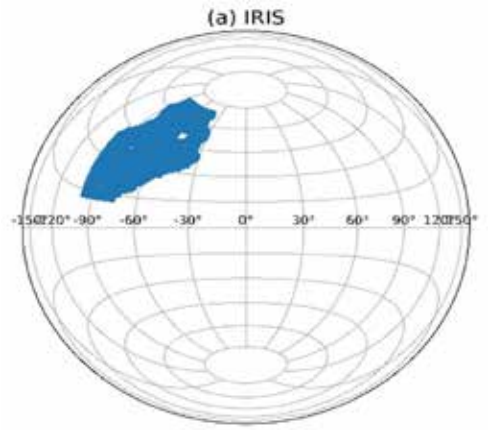

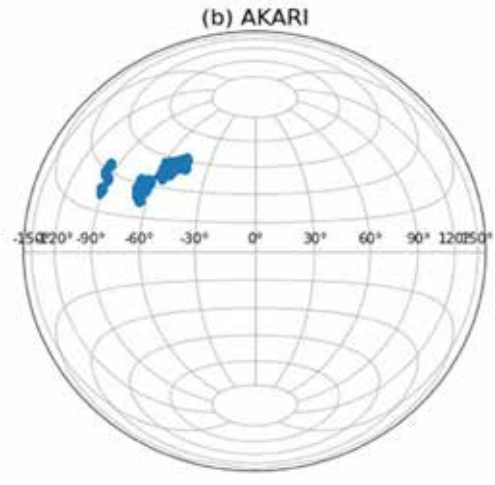

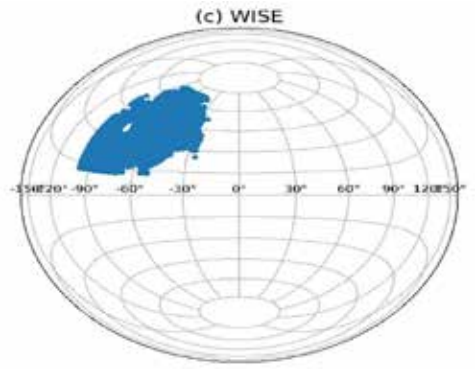

Figure 1. Projection map of the source (a) IRIS, (b) AKARI, and (c) WISE survey.

The position of our candidate in the entire galactic sphere as shown by the IRIS, AKARI, and WISE maps is shown in Figure 1 (a), (b), and (c). The candidate is located in northern hemisphere.

A linear Fitting of Flux

A best-fit line between IRIS F100 µm and F60 µm, AKARI F140 µm and F90 µm, and WISE F12 µm and F22 µm along the X-axis and Y-axis, respectively, represents the flux distribution in Figure 2 (a), (b), and (c). The greatest flux density zone is used to depict the most occupied area. In the context of IRIS, the flux is linearly distributed, and the slope, intercept, and correlation coefficient (r) are all calculated to be 0.320, -12.500, and 0.820 respectively.

In AKARI, the flux is more concentrated in the middle, and the slope, intercept, and correlation coefficient (r) are all calculated to be 0.079, 69.880 and 0.420 respectively. In WISE, the flux is more concentrated in the lower left, and the slope, intercept, and correlation coefficient (r) are all calculated to be 0.026, 126.83, and 0.608 respectively. The key benefit of finding the best fit in various pixels is that it provides the ratio of lower flux to higher flux (R), which aids in determining the structure's temperature.

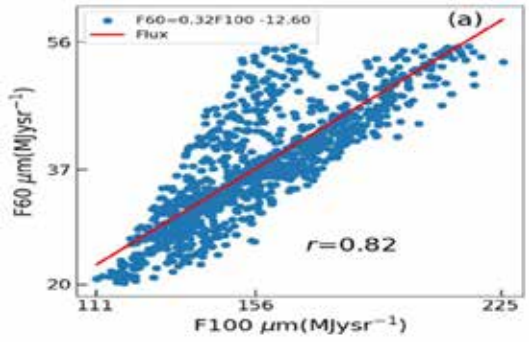

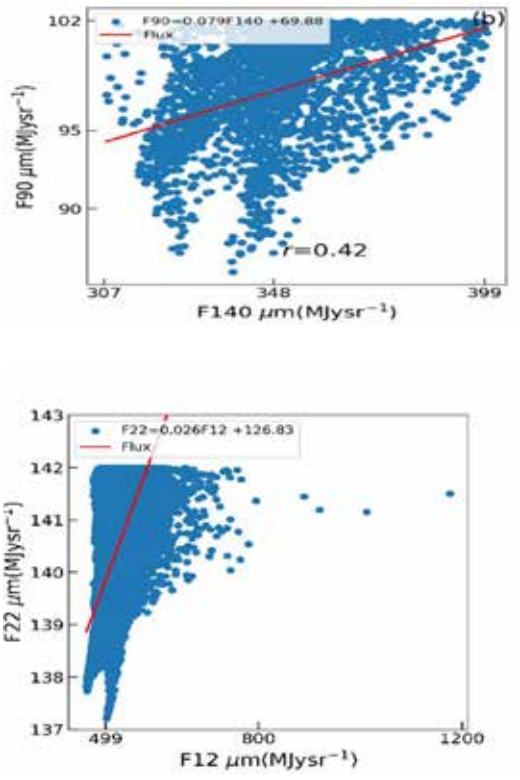

Figure 2. Scatter plots with linear best fit (a) IRIS: F100 μm vs F60 μm, (b) AKARI: F140 μm vs 90 μm, and (c)WISE: F12 μm vs F22 μm. The dots indicate the flux, whereas the straight line provides the best fit line.

Distribution of Dust Temperature

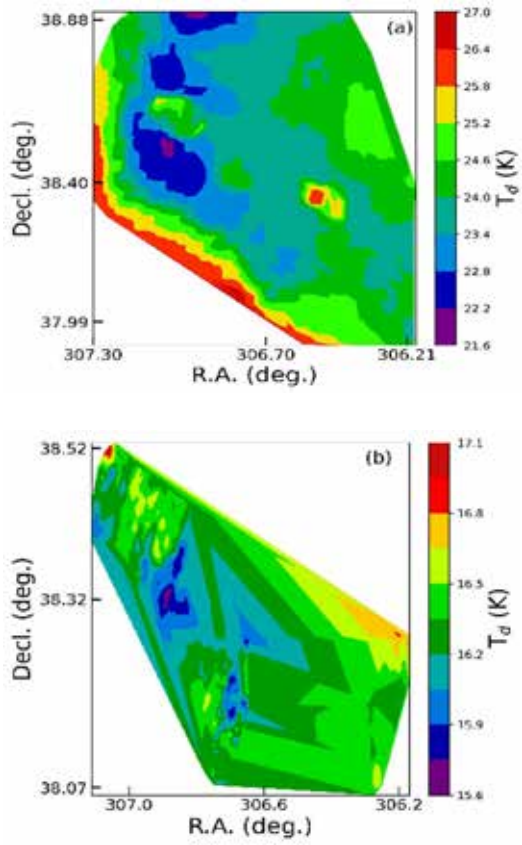

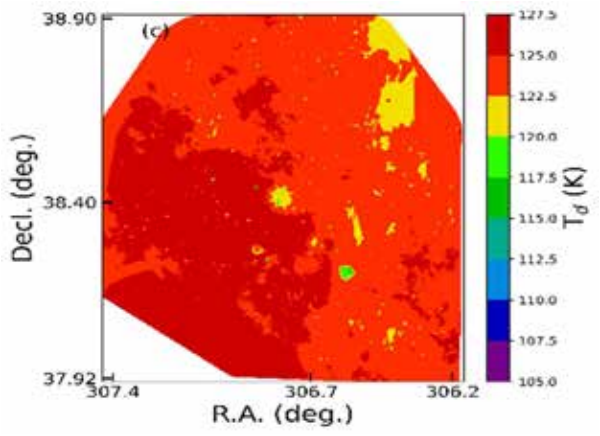

Figure 3. The contour plot of (a) IRIS: R.A. vs Decl. versus Temperature (b) AKARI: R.A. vs Decl. versus Temperature (c) WISE: R.A.vs Decl. vs Temperature at R.A.= 19^h 57^m 48.449^s , Decl. = $+33^0$ 41^m 21.25^s. The colour bar indicates the value of temperature.

The contour map of temperature fluctuation from the IRIS, AKARI, and WISE surveys is shown in Figure 3 (a), (b), and (c). The IRIS survey determined that the average temperature was 24.230±0.229 K, with a maximum temperature of 24.930±0.229 K in some areas of the outside region and a minimum of 23.770±0.229 K in areas closer to the core. Similar to this, the average temperature in the AKARI survey was found to be 16.780±0.890 K with maximum temperature of 17.710±0.890 K in the center and minimum temperature of 16.780±0.890 K in the outer region. The maximum, minimum and average temperature in the AKARI survey were 125.110±0.430 K, 122.550±0.430 K and 123.750±0.430 K respectively. Here the red colour shows the maximum temperature whereas the violet colour indicates minimum temperature.

Distribution of Dust Mass

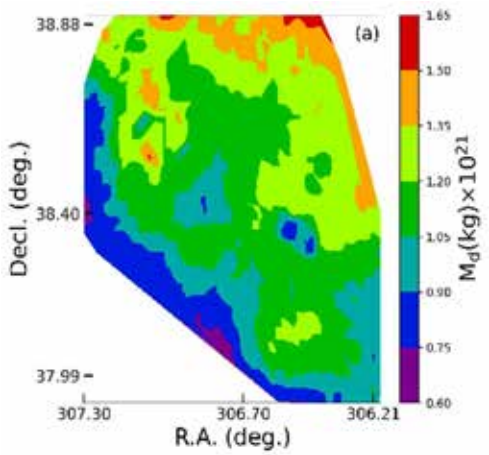

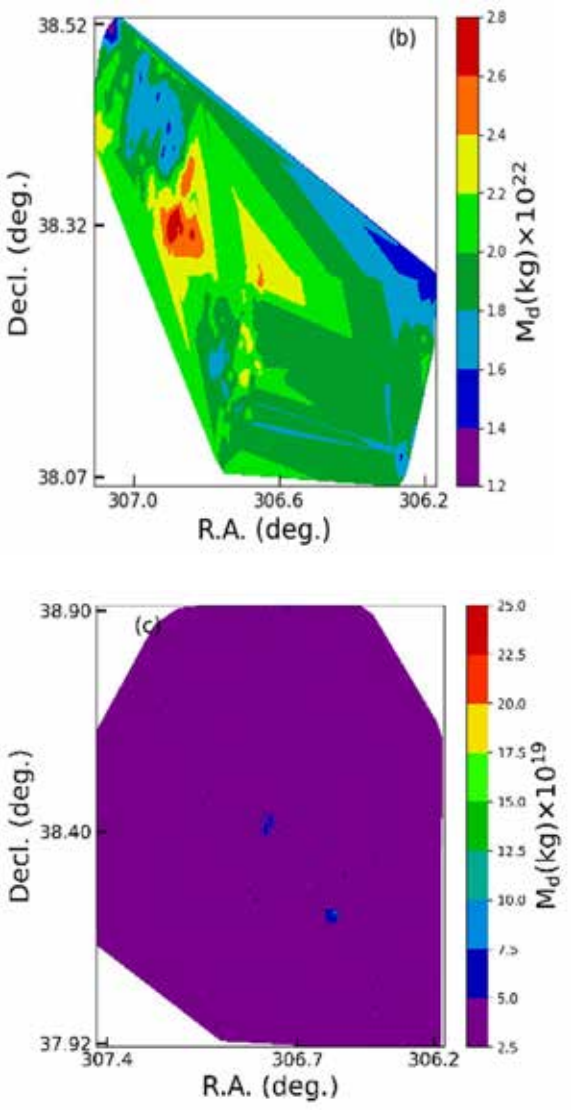

Figure 4. The contour plot of (a) IRIS: R.A. vs Decl. Versus Dust Mass (b) AKARI: R.A. vs Decl. vs Dust Mass (c) WISE: R.A. vs Decl. vs Dust Mass at R.A.= $19^h\ 57^m\ 48.449^s$, Decl. =$+33^0\ 41^m\ 21.25^s$. The colour bar indicates the value of dust mass.

The contour map of the dust mass variation is shown in the Figure 4 (a) IRIS (b) AKARI and (c)WISE surveys. The average mass was found as 1.120×10^{20} kg, 1.930×10^{22} kg and 3.790×10^{19}kg in IRIS, AKARI, and WISE respectively. The colour bar indicates that the distribution of mass is greatest in the core region and least in the outer region in all three surveys. In the IRIS survey, the maximum mass and minimum mass was found to be 1.600×10^{21} kg and 7.010×10^{20} kg respectively. Likewise, the maximum and minimum mass in AKARI survey was found to be 2.730×10^{22} kg and 1.290×10^{22} kg respectively. The maximum and minimum value of dust mass was found to be 2.290×10^{20} kg and 3.010×10^{19} kg respectively.

Planck's Function distribution

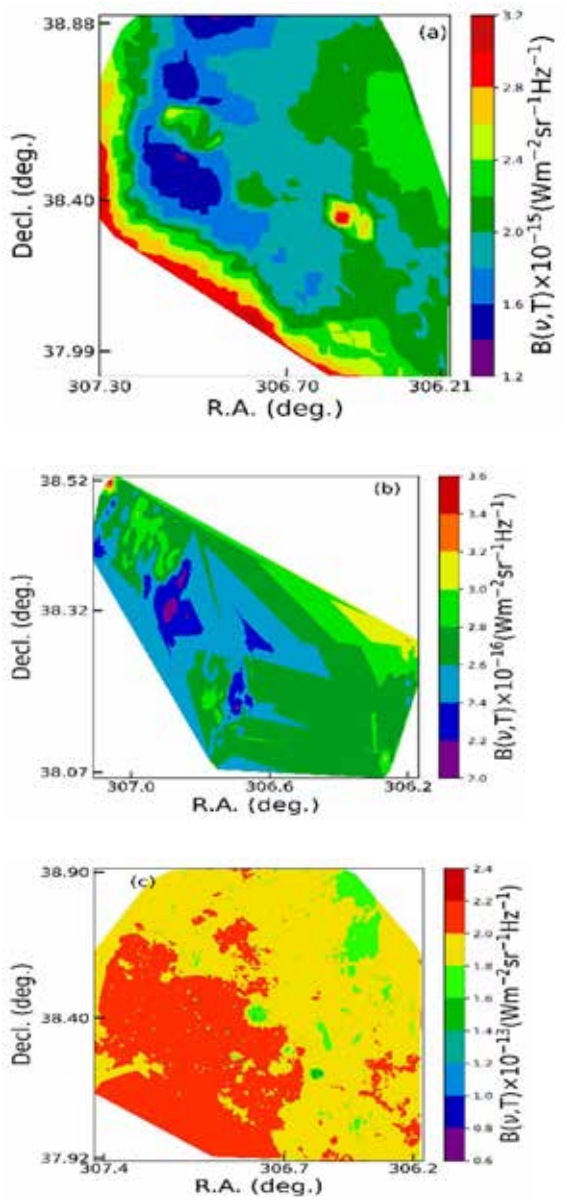

Figure 5. The contour plot of (a) IRIS: R.A. vs Decl. vs Planck's Function (b) AKARI: R.A. vs Decl. vs Planck's Function (c) WISE: R.A. vs Decl. vs Planck's Function at R.A.= $19^h\ 57^m\ 48.449^s$, Decl. =$+33^0\ 41^m\ 21.25^s$. The colour bar indicates the value of Planck's Function.

Figure 5 (a), (b) and (c) shows the Planck's function variation in the IRIS, AKARI, and the WISE survey. The Planck function depicts the spectrum density of electromagnetic radiation emitted by a body at a given temperature. The spectral density increases from violet to red as indicated by the colour bar. We can readily analyze the plot to determine that the region with higher flux density also has higher spectral density, and vice versa. In IRIS survey the maximum value of the spectral density was

found to be 1.240 $\times 10^{-15}$W$m^{-2}sr^{-1}Hz^{-1}$ and that of minimum value found to be 9.360$\times 10^{-1}$ W$m^{-2}sr^{-1}Hz^{-1}$. Similarly, in AKARI survey, we have calculated the maximum value of spectral density to be 4.370 $\times 10^{-16}$W$m^{-2}sr^{-1}Hz^{-1}$ and minimum value as 1.907 $\times 10^{-16}$W$m^{-2}sr^{-1}Hz^{-1}$. In the case of WISE survey, the maximum and minimum value of the spectral density was found to be 2.011$\times 10^{-1}$ W$m^{-2}sr^{-1}Hz^{-1}$ and 1.800$\times 10^{-13}$W$m^{-2}sr^{-1}Hz^{-1}$ respectively.

Comparison with previous work

Table1: Comparison of the dust temperature and mass of previous work.

Previous work	Source	Survey	Minimum Temp. (K)	Maximum Temp. (K)	Dust Mass (kg)
Gautam et al.[11]	AGB	IRAS	21.6± 0 .09	22.5± 0.09	5.93× 10^{25}
Gautam et al.[12]	AGB	IRAS	19.7± 0 .35	21.1 ± 0.35	1.86× 10^{28}
Gautam et al.[13]	AGB	IRAS	21.4	21.9	4×10^{27}
Joshi et al.[15]	WD 1334-678	IRAS	17.70± 0.01	18.81± 0.01	1.1× 10^{25}
This Work	IRAS 19558+333	IRIS, AKARI, and WISE	(IRIS) 23.77±0 .22 (AKARI) 16.78 ±0.89 (WISE) 122.55±0.43	(IRIS) 24.93±0.22 (AKARI) 17.71± 0.89 (WISE) 125.11± 0.43	(IRIS) 1.5×10^{29} (AKARI) 1.38×10^{30} (WISE) 6.27×10^{27}

We have got the similar result of dust mass and temperature in our study.

Conclusions

The main aim of our experiment is to study the physical properties around AGB star such as dust mass estimation, dust color temperature, plank's function, and determining the type of AGB star and their relation around it. We have used three different surveys: IRIS, AKARI and WISE at different wavelength and studied three different structures around the AGB star. Following are the conclusion that can be drawn from our study.

- The dust color temperature is found in the range between 23.770 ± 0.229 K to 24.230 ± 0.229 K in IRIS survey, 15.496 ± 0.190 K to 16.775 ± 0.019 K in AKARI survey and 122.550 ± 0.430 K to 125.119 ± 0.043 K in WISE survey. The dust color temperature is higher in WISE as it has inverse relation with flux. From the lower value of standard error, it is concluded the star is in early AGB phase and the low temperature difference suggest it to be in thermal equilibrium.
- The minimum and maximum dust mass is found to be 1.606 × 10^{21} kg (8.030× 10^{-10} M⊙) and 7.013×10^{20} kg (3.506× 10^{-10} M⊙) in IRIS; 2.739×10^{22} kg (1.369 × 10^{-8} M⊙) and 1.292×10^{22} kg (6.460× 10^{-9} M⊙) in AKARI and 2.297 × 10^{20} kg (1.148 × 10^{-10} M⊙) and 3.013× 10^{19} kg (1.506 × 10^{-11} M⊙) in the WISE surveys respectively. The value of dust mass is higher in WISE as it has direct relation with flux.
- The average visual extinction is found to be 8.190 ×10^{-13} mag. in IRIS, 7.280 × 10^{-12} mag. in AKARI and 8.370 × 10^{-15} mag in WISE survey. We obtained a negative correlation coefficient, implying an inverse relationship between visual extinction and dust temperature. Such a low correlation value indicates a rapidly fluctuating nature attempting to find equilibrium.

- The flux density is low in the middle part of the selected cavity of C-rich AGB star. This might be due to the presence of external factor.

Acknowledgements

We are grateful to the Department of Physics, Amrit Campus, and the Central Department of Physics, Tribhuvan University for giving us the opportunity to work in this scientific field. This study made use of the Gaia Archive, SIMBAD data base, SkyView Virtual Observatory, IRIS survey, AKARI survey, and WISE survey.

References

[1] Saintonge, A. and Catinella, B. 2022. The cold interstellar medium of galaxies in the Local Universe. *Annual Review of Astronomy and Astrophysics*. **60**: 319-361. https://doi.org/10.1146/annurev-astro-021022-043545

[2] Pagel, B. E. J. and Edmunds, M. G. 1981. Abundances in stellar populations and the interstellar medium in galaxies. *Annual Review of Astronomy and Astrophysics*. **19**(1). 77-113. https://doi.org/10.1146/annurev.aa.19.090181.000453

[3] Hollenbach, D. J. and Tielens, A. G. G. M. 1999. Photodissociation regions in the interstellar medium of galaxies. *Reviews of Modern Physics*. **71**(1): 173. https://doi.org/10.1103/RevModPhys.71.173

[4] Suh, K. W. and Kwon, Y. J. 2009. A Catalog of AGB Stars in IRAS psc. *Journal of the Korean Astronomical Society*. **42**(4): 81-91. https://doi.org/10.5303/JKAS.2009.42.4.081

[5] Marigo, P., Girardi, L., Bressan, A., Groenewegen, M. A., Silva, L. and Granato, G. L. 2008. Evolution of asymptotic giant branch stars-II. Optical to far-infrared isochrones with improved tp-agb models. *Astronomy & Astrophysics*. **482**(3): 883-905. https://doi.org/10.1051/0004-6361:20078467

[6] Suh, K. W. 2020. Infrared Properties of Asymptotic Giant Branch Stars in Our Galaxy and the Magellanic Clouds. *The Astrophysical Journal*. **891**(1): 43. 10.3847/1538-4357/ab6609

[7] Jha, A.K. and Aryal, B. 2017. A Study of a Cavity Nearby a Pulsar at-60º Latitude in the Far Infrared Map. *Journal of Nepal Physical Society.* **4**(1):33-41.

[8] Jha, A.K. and Upadhyay, D.R. 2017. Dust Structure around two Asymptotic Giant Stars at Latitude 32° and 40.67°. *Himalayan Physics*. **6 and 7**: 41-47.

[9] Jha, A.K., Aryal, B. and Weinberger, R. 2017. A study of dust color temperature and dust mass distributions of four far infrared loops. *Revista mexicana de astronomía y astrofisica*. **53**: 467-476.

[10] Jha, A.K. and Aryal, B. 2018. Dust color temperature distribution of two FIR cavities at IRIS and AKARI maps. *Journal of Astrophysics and Astronomy*. **39**(2): 1-7.

[11] Gautam, A. K. and Aryal, B. 2019. Study of far infrared cavity around a post AGB star under IRAS survey at galactic latitude-3°. *BIBECHANA*. **16**: 23-30. https://doi.org/10.3126/bibechana.v16i0.20960

[12] Gautam, A. K. and Aryal, B. 2020. Study of dust color temperature and visual extinction distribution of a far infrared cavity at 60 and 100 μm IRAS map around the AGB star at galactic latitude 8.6 º. *BIBECHANA*. **17**: 42-49. https://doi.org/10.3126/bibechana.v17i0.25839

[13] Gautam, A. K. and Aryal, B. 2019. Study of a Far Infrared Cavity around an AGB Star under Iras Survey at Galactic Latitude-1.6°. *Journal of Nepal Physical Society*. **5**(1): 35-41. https://doi.org/10.3126/jnphyssoc.v5i1.26929

[14] Gautam, A. K. and Chhatkuli, D. N. 2020. Planck Function Distribution in the Far Infrared Cavity nearby AGB Star at Galactic Latitude 0.6 º. *Journal of Nepal Physical Society*. **6**(2): 97-103. https://doi.org/10.3126/jnphyssoc.v6i2.34864

[15] Joshi, I. N., Jha, A. K. and Aryal, B. 2021. A study of dust structure nearby white dwarf WD1334-678. *BIBECHANA*. **18**(2): 130-137. https://doi.org/10.3126/bibechana.v18i2.37439

[16] Dupac X, Bernard JP, Boudet N, Giard M, Lamarre JM, Mény C, et al. 2003. Inverse temperature dependence of the dust submillimeter spectral index. *Astronomy & Astrophysics*.,**404**(1): L11–L15. 10.1051/0004-6361:20030575

[17] Schnee, S.L., Ridge, N.A., Goodman. A.A. and Li. J.G. 2005. A complete look at the use of IRAS emission maps to estimate extinction and dust temperature. *The Astrophysical Journal*. **634**(1): 442. 10.1086/491729

[18] Mennella, V., Colangeli, L. and Bussoletti, E. 1995. The absorption coefficient of cosmic carbon analogue grains in the wavelength range 20-2000 microns. *Astronomy and Astrophysics*, **295**: 165-170.

[19] Tiwari, M., Gautam, S. P., Silwal, A., Subedi, S., Paudel, A. and Jha, A. K. 2020. Study of Dust Properties of two Far Infrared Cavities near by Asymptotic Giant Branch stars under Infrared Astronomical Satellite Maps. *Himalayan Physics*. **9**:60-71. https://doi.org/10.3126/hp.v9i01.40193

[20] Hildebrand RH. The determination of cloud masses and dust characteristics from submillimetre thermal emission. 1983.

[21] Chaudhary, A., Thapa, B., Sodari, T., Chaudhary, K. and Upadhyay, D. R. 2022. Distribution of Dust Color Temperature, Planck's Function, and Dust Mass around PSR J1240-4124. *Journal of Nepal Physical Society*, **8**(1): 88–95. https://doi.org/10.3126/jnphyssoc.v8i1.48292